Analysis of the Piezoelectric Performance of Modern 0–3-Type Composites Based on Relaxor-Ferroelectric Single Crystals

VITALY YU. TOPOLOV,[1]* PAOLO BISEGNA,[2] AND CHRISTOPHER R. BOWEN[3]

[1] Department of Physics, Southern Federal University, 5 Zorge Street, 344090 Rostov-on-Don, Russia

[2] Department of Civil Engineering, University of Rome "Tor Vergata", 00133 Rome, Italy

[3] Materials Research Centre, Department of Mechanical Engineering, University of Bath, BA2 7AY Bath, United Kingdom

Abstract

Effective piezoelectric coefficients e_{33}^*, d_{33}^*, g_{33}^*, *and* h_{33}^*, *squared figures of merit* $d_{33}^* g_{33}^*$ *and* $d_h^* g_h^*$, *and other related parameters of novel 0–3 and 0–3–0 composites based on single crystals of relaxor-ferroelectric solid solutions of* $(1-x)Pb(Mg_{1/3}Nb_{2/3})O_3 - xPbTiO_3$ *are studied using the effective field method, effective medium method and finite element method. The volume-fraction dependences of a number of parameters and figures of merit are determined using the above methods and compared for composites with aligned prolate spheroidal inclusions. Four parameter ratios that determine interconnections between the effective electromechanical constants of the 0–3-type composites are first introduced. These parameter ratios are used to interpret the longitudinal dielectric and piezoelectric response of composite structures with prolate inclusions that exhibit high piezoelectric activity. The role of piezoelectric anisotropy and activity of the composite components in forming the longitudinal piezoelectric effect is analysed. Specific novel composite architectures with high piezoelectric sensitivity (longitudinal and hydrostatic) are identified and discussed.*

Keywords Composite; piezoelectric coefficients; spheroidal inclusion; relaxor-ferroelectric single crystal; relaxor-ferroelectric ceramic

PACS: 77.65.-j: Piezoelectricity and electromechanical effects; 77.84.Lf: Composite materials; 77.84.-s: Dielectric, piezoelectric, ferroelectric, and antiferroelectric materials

Title for the running head: **Piezoelectric Performance of 0–3-Type Composites**

* Corresponding author. E-mail: vutopolov@sfedu.ru

1. Introduction

Piezo-active composites often show a remarkable ability to convert mechanical energy into electric energy and vice versa. In the last decades these materials have been studied and developed [1, 2] in an attempt to improve their performance for sensor, hydrophone and other applications. The application of single crystals (SCs) of perovskite-type relaxor-ferroelectric $(1 - x)Pb(Mg_{1/3}Nb_{2/3})O_3 - xPbTiO_3$ (PMN–*x*PT) and $(1 - y)Pb(Zn_{1/3}Nb_{2/3})O_3 - yPbTiO_3$ (PZN–*y*PT) solid solutions as highly effective components of novel piezo-active composites has been discussed in recent papers (see, for instance, Refs. 2–6). The use of SCs with 'engineered domain structures' [7] and compositions near the morphotropic phase boundary [7–9] are of significant interest due to their excellent electromechanical properties compared to those of conventional piezoelectric ceramics [2, 10]. Results on the relaxor-ferroelectric SC / polymer composites with 2–2 [11–14], 1–3 [3–6, 15, 16] and 0–3 [17] connectivity patterns (in terminology of Newnham et al. [18]) show that the domain-engineered PMN–*x*PT and PZN–*y*PT SCs promote high piezoelectric sensitivity, activity and significant hydrostatic piezoelectric response within specific ranges of volume fractions of components. The role of the relaxor-ferroelectric SC as a component in 1–3-type composites has also been analysed [4] to demonstrate the volume fraction ranges in which the effective composite parameters are most sensitive to material properties and composite architecture. Related 0–3 SC / polymer composites and maxima of their effective parameters were considered in paper [17]. At present it is not yet fully understood how the SC component influences the piezoelectric response of 0–3 composites with isolated ferroelectric inclusions that are surrounded by a matrix with piezoelectric properties (e.g., ferroelectric ceramic or polymer). This work is concerned with a prediction of the effective piezoelectric properties of the 0–3-type composites based on PMN–*x*PT SCs.

In the present paper we discuss features of the performance of the 0–3-type SC-based composites for piezoelectric sensor and related applications. To compare the performance and

identify potential novel architectures, we consider composites that contain SC inclusions embedded in one of the following matrices: polymer, porous ceramic or monolithic ceramic. For comparison, the effective electromechanical properties of the piezo-active composites are predicted using different methods, and an emphasis is placed on the piezoelectric coefficients that characterise the longitudinal response of the studied composites on the poling direction.

2. Methods for Modelling of Effective Electromechanical Properties

In this study we consider composites with the spheroidal SC inclusions (Fig. 1) that are uniformly aligned in the matrix and form a periodic structure. In each inclusion the main crystallographic axes are oriented as follows: $X \parallel OX_1$, $Y \parallel OX_2$ and $Z \parallel OX_3$. It is assumed that centres of symmetry of the inclusions occupy sites of a simple lattice with unit-cell vectors parallel to the OX_j axes shown in Fig. 1. The SC inclusions have a spontaneous polarisation $\boldsymbol{P}_s^{(1)} \parallel Z \parallel OX_3$, and the composite sample as a whole is poled along the OX_3 axis. The composite is characterised by 0–3 connectivity in case of the monolithic matrix and by 0–3–0 connectivity in the case of a porous matrix (3–0 connectivity) with a system of isolated air inclusions. It is assumed that the spherical air inclusions are uniformly distributed in the ceramic matrix and the radius of each air inclusion is much less than the length of each semiaxis a_j of the spheroidal inclusion.

To determine the effective electromechanical properties of the 0–3-type composite with the above-described microgeometry, it is possible to apply averaging procedures [2, 19–21], that allow for an electromechanical interaction between the piezo-active SC inclusions in the composite matrix. The first procedure is based on the effective field method (EFM), i.e., the Mori – Tanaka method [22] generalised for heterogeneous piezoelectric media [19–21]. In the EFM, an individual inclusion within the matrix, which is under an external electroelastic field, is subjected to the action of an unknown average (so-called effective) electroelastic field. This average field is a result of the external field applied to the matrix (and, therefore, to the composite sample as a whole) wherein the interaction between the inclusions plays the key role. The second procedure is

based on the effective medium method (EMM). In the EMM, a single inclusion is considered to be surrounded by a homogenised (effective) medium, and this medium is regarded as a matrix with similar inclusions. The EFM and EMM represent two self-consistent schemes for the calculation of the full set of electromechanical constants, and the electromechanical interaction between the inclusions in the matrix plays a key role in determining the effective properties. Using the equivalent inclusion approach, the coupled electroelastic behaviour of the 0–3 ferroelectric ceramic / polymer composite with spheroidal inclusions has been previously modelled [19–23] in a wide range of the volume fraction *m*.

The effective electromechanical properties of the 0–3-type composite are represented in the general form [2, 24] as

$$|| C^* || = || C^{(2)} || + m (|| C^{(1)} || - || C^{(2)} ||) || A ||, \quad (1)$$

where $|| C^{(n)} || = \begin{pmatrix} || c^{(n),E} || & || e^{(n)} ||^t \\ || e^{(n)} || & -|| \varepsilon^{(n),\xi} || \end{pmatrix}$ is the 9 × 9 matrix that characterises the electromechanical properties of the inclusions (n = 1) and the surrounding medium (n = 2) in the 0–3 composite, $|| A ||$ is the mechanical strain – electric field concentration matrix (9 × 9 matrix), $|| c^{(n),E} ||$ is the 6 × 6 matrix of elastic moduli measured at constant electric field, $|| e^{(n)} ||$ is the 6 × 3 matrix of piezoelectric coefficients, $|| \varepsilon^{(n),\xi} ||$ is the 3 × 3 matrix of dielectric permittivities measured at constant mechanical strain, and superscript *t* denotes the transposition. The matrix ||*A*|| from Eq. (1) is related to the boundary conditions in the 'inclusion – surrounding medium' region and written [2, 19, 21, 24] as follows:

$$|| A || = [|| I || + (1 - m) || S || || C^{(2)} ||^{-1} (|| C^{(1)} || - || C^{(2)} ||)]^{-1} \quad (2)$$

(EFM) or

$$|| A || = [|| I || + || S || \, || C^* ||^{-1} (|| C^{(1)} || - || C^* ||)]^{-1} \quad (3)$$

(EMM), where $|| I ||$ is the 9 × 9 identity matrix, $|| S ||$ is the 9 × 9 matrix containing components of the Eshelby electroelastic tensor [19, 21, 24] and $|| C^* ||$ is the 9 × 9 matrix from Eq. (1). Elements of $|| S ||$ from Eqs. (2) and (3) depend on electromechanical constants of the matrix of the 0–3 composite and on the aspect ratio $\rho = a_1 / a_3$ of the SC spheroidal inclusions. In the EMM, effective electromechanical constants are calculated as a result of a series of iterations involving Eqs. (3) and (1). Electromechanical constants of the porous ceramic matrix with 3–0 connectivity are determined from an expression used in the dilute approach [25]

$$|| C^{(2)} || = || C^{(FC)} || \, [|| I || - m_p \, ([|| I || - (1 - m_p) \, || S ||)^{-1}], \quad (4)$$

where $|| C^{(FC)} ||$ describes the electromechanical properties of monolithic ceramic, m_p is the volume fraction of the air inclusions (i.e., porosity of the ceramic matrix in the composite sample) and $|| S ||$ is calculated by taking into account elements of $|| C^{(FC)} ||$ and the shape of the air inclusions ($\rho = 1$). In the case of the 0–3–0 composite matrix, $|| C^{(2)} ||$ from Eq. (4) is then substituted into Eq. (1) and taken into account when determining $|| A ||$ and $|| S ||$ from Eqs. (2) and (3).

In the present study the COMSOL package [26] is applied to obtain the volume-fraction dependence of the effective electromechanical properties of the 0–3 composite based on a SC with high piezoelectric activity. In particular, a unit cell, containing the spheroidal inclusion (Fig. 1) with radius adjusted to yield the appropriate volume fraction *m*, is discretised using tetrahedral elements. Their number, depending on the aspect ratio ρ of the spheroidal inclusion, varies from 320,000 to 760,000. The unknown displacement and electric-potential fields are interpolated using linear Lagrangian shape functions. The corresponding number of degrees of freedom varies from

200,000 to 500,000. Periodic boundary conditions are enforced on the boundary of the unit cell, and the matrix of effective constants of the composite is computed column-wise, performing calculations for diverse average strain and electric fields imposed to the structure. The Geometric Multigrid [27] iterative solver (V-cycle, successive over-relaxation pre- and post-smoother, direct coarse solver) is employed. After solving the electro-elastic equilibrium problem, the effective electromechanical constants of the 0–3-type composite are computed, by averaging the resulting local stress and electric-displacement fields over the unit cell.

In the three aforementioned methods, the effective properties of the composite are determined in a long-wave approximation [2], i.e., in a case when the wavelength of an external acoustic field is much longer than the semi-axes a_1 and a_3 of the separate inclusion (Fig. 1). The matrix of the effective electromechanical properties $\| C^* \| = \begin{pmatrix} \| c^{*E} \| & \| e^* \|^t \\ \| e^* \| & -\| \varepsilon^{*\xi} \| \end{pmatrix}$ is calculated as a function of m and ρ (0–3 composite), or m, ρ and m_p (0–3–0 composite). The interrelationships of the effective piezoelectric coefficients e^*_{fq} (stress coefficients), d^*_{fq} (charge coefficients), g^*_{fq} (voltage coefficients), and h^*_{fq} (strain coefficients) are expressed by a set of equalities [28] as follows:

$$d^*_{fp} = \varepsilon^{*\sigma}_{fk}\, g^*_{kq} = e^*_{fq}\, s^{*E}_{qp}, \tag{5}$$

$$e^*_{fp} = \varepsilon^{*\xi}_{fk}\, h^*_{kp} = d^*_{fq}\, c^{*E}_{qp}, \tag{6}$$

$$g^*_{fp} = \beta^{*\sigma}_{fk}\, d^*_{kp} = h^*_{fq}\, s^{*D}_{qp}, \tag{7}$$

and

$$h^*_{fp} = \beta^{*\xi}_{fk}\, e^*_{kp} = g^*_{fq}\, c^{*D}_{qp}. \tag{8}$$

In Eqs. (5) – (8) $\varepsilon_{fk}^{*\sigma}$ is dielectric permittivity measured at constant mechanical stress, s_{qp}^{*E} and s_{qp}^{*D} are elastic compliances measured at constant electric field and electric displacement, respectively, c_{qp}^{*D} is elastic modulus measured at constant electric displacement, and $\beta_{fk}^{*\sigma}$ and $\beta_{fk}^{*\xi}$ characterise dielectric impermeability at constant stress and strain, respectively. Electromechanical constants from Eqs. (5) – (8) are also linked [28] by the following equalities:

$$\varepsilon_{kr}^{*\sigma} - \varepsilon_{kr}^{*\xi} = d_{kf}^{*}\, e_{rf}^{*}, \tag{9}$$

$$c_{pq}^{*D} - c_{pq}^{*E} = e_{fp}^{*}\, h_{fq}^{*}, \tag{10}$$

$$s_{pq}^{*D} - s_{pq}^{*E} = d_{fp}^{*}\, g_{fq}^{*}, \tag{11}$$

and

$$\beta_{kr}^{*\xi} - \beta_{kr}^{*\sigma} = g_{kf}^{*}\, h_{rf}^{*}. \tag{12}$$

Taking into account electromechanical constants from Eqs. (5) – (8), one can consider dependences of a series of effective parameters on volume fractions of components and on the aspect ratios of the inclusions and porosity of the ceramic. The important composite parameters and figures of merit to be studied include the electromechanical coupling factors $k_{33}^{*} = d_{33}^{*} / (s_{33}^{*E}\, \varepsilon_{33}^{*\sigma})^{1/2}$ (longitudinal factor) and $k_{t}^{*} = e_{33}^{*} / (c_{33}^{*D}\, \varepsilon_{33}^{*\xi})^{1/2}$ (thickness factor) and squared figures of merit $(Q_{33}^{*})^2 = d_{33}^{*}\, g_{33}^{*}$ (at the longitudinal piezoelectric response) and $(Q_{h}^{*})^2 = d_{h}^{*}\, g_{h}^{*}$ (at the hydrostatic piezoelectric response), where $d_{h}^{*} = d_{33}^{*} + 2\, d_{31}^{*}$ and $g_{h}^{*} = g_{33}^{*} + 2\, g_{31}^{*}$ are hydrostatic piezoelectric coefficients of the composite. Electromechanical coupling factors characterise ability of any piezoelectric material to convert electric energy into mechanical energy and vice versa at different oscillation modes [10, 28]. Figures of merit are often used [1, 2, 11, 12, 15, 16] to

describe the sensor signal-to-noise ratio of the piezoelectric element and to characterise its piezoelectric sensitivity.

3. Results and Discussion

3.1. Effective Piezoelectric Coefficients and Their Anisotropy

To predict the performance of the studied 0–3-type composites, we use complete sets of experimental electromechanical constants [9, 29, 30] involved in $\| C^{(n)} \|$ from Eqs. (1) – (4). Room-temperature constants of components of the 0–3 SC-based composites considered in this paper are collected in Table 1. Compositions of PMN–*x*PT were chosen near the morphotropic phase boundary due to high piezoelectric activity ($d_{3j} \sim 10^3$ pC / N). At room temperature PMN–0.33PT is SC with a rhombohedral distortion of the perovskite unit cell (3*m* symmetry). However, the domain-engineered PMN–0.33PT SC poled along the perovskite unit-cell direction [001] is characterised by macroscopic 4*mm* symmetry. In this polydomain state, there are four domain types that provide the effective spontaneous polarisation $\boldsymbol{P}_s^{(1)} \| OX_3$ of the SC sample as a whole. Electromechanical constants of porous ceramic of PMN–0.35PT were calculated using data on poled monolithic ceramic (see Table 1) and Eq. (4). Both the monolithic and porous ceramics in the poled state are characterised by ∞*mm* symmetry. Contrary to the SC and ceramic components, araldite is the isotropic piezo-passive polymer material. The electromechanical constants listed in Table 1 indicate that the anisotropy of the piezoelectric coefficients e_{3j} is considerable: for example, $e_{33} / |e_{31}| = 5.2$ for PMN–0.33PT SC, $e_{33} / |e_{31}| = 5.6$ for monolithic ceramic of PMN–0.35PT and $e_{33} / |e_{31}| = 10.4$ for porous ceramic of PMN– 0.35PT.

Below we analyse piezoelectric features of the following 0–3-type SC-based composites: PMN–0.33PT SC / araldite (*composite 1* in our notations), PMN–0.33PT SC / PMN–0.35PT ceramic (*composite 2* in our notations) and PMN–0.33PT SC / PMN–0.35PT porous ceramic at $m_p = 0.3$ (*composite 3* in our notations). In an attempt to attain large absolute values of the

longitudinal piezoelectric coefficients X_{33}^{*} (X = e, d, g, and h) in these anisotropic structures and to weaken the depolarising electric field in the presence of SC inclusions, we consider composites with the prolate inclusions ($0 < \rho < 1$). The results, shown in Figs. 2 – 4, suggest that the prolate shape of the SC inclusion with the lower ρ value promotes a higher composite piezoelectric activity at m = const. This prolate geometry is also favourable in attaining high piezoelectric sensitivity ($g_{33}^{*} = d_{33}^{*} / \varepsilon_{33}^{*\sigma}$) in composite 1 due to the large piezoelectric coefficient d_{33}^{*} combined with a relatively low dielectric permittivity $\varepsilon_{33}^{*\sigma}$ in the volume-fraction range $0 < m < 0.1$.

The reason for the difference between the values of the piezoelectric coefficients X_{33}^{*} calculated for composite 1 by means of different methods (Fig. 2 (*a*) – (*d*)) is possibly due to a relatively small ratio of the elastic constants of the SC and polymer and the large ratio of their dielectric constants. This may also explain the difference between values of dielectric permittivity $\varepsilon_{33}^{*\xi}$ (Fig. 2 (*e*)). The matrix of effective constants || C* || contains the piezoelectric coefficients e_{ij}^{*}, elastic moduli c_{ab}^{*E} and dielectric permittivities $\varepsilon_{pp}^{*\xi}$, and these constants are obtained directly from averaging (see Eqs. (1) – (4)). According to our evaluations involving constants of PMN–0.33PT SC and araldite (see Table 1), the ratios $c_{11}^{(1),E} / c_{11}^{(2)} = 14.7$ and $c_{33}^{(1),E} / c_{11}^{(2)} = 13.2$ are order-of-magnitude less than $\varepsilon_{33}^{(1),\xi} / \varepsilon_{33}^{(2)} = 170$. This condition leads to a significant re-distribution of internal electric and mechanical fields in the 0–3 PMN–0.33PT SC / araldite composite and leads us to believe that EFM could be applied with some restrictions for 0–3 connectivity. We note for comparison that the similar mutual arrangement of curves $e_{33}^{*}(m)$ and $d_{33}^{*}(m)$ from the EFM, FEM and EMM data [21] takes place in case of the 0–3 ferroelectric ceramic / polymer composite. For its components ratios $c_{11}^{(1),E} / c_{11}^{(2)} \approx 19$, $c_{33}^{(1),E} / c_{11}^{(2)} \approx 16$ and $\varepsilon_{33}^{(1),\xi} / \varepsilon_{33}^{(2)} \approx 110$ hold and the order-of-magnitude distinction between dielectric constants is again attained. However, it should be noted, that in recent paper [31] on the 1–3 $PbTiO_3$-type ceramic / polymer composite with circular

cylindrical inclusions (i.e., in case of ρ = 0), good agreement between the parameters calculated using the EFM and FEM is attained in a wide volume-fraction range. The 1–3 composite consists of components, for which ratios $c_{11}^{(1),E}/c_{11}^{(2)} \approx 24$, $c_{33}^{(1),E}/c_{11}^{(2)} \approx 23$ and $\varepsilon_{33}^{(1),\xi}/\varepsilon_{33}^{(2)} \approx 31 \ldots 37$ [31] are true and no aforementioned order-of-magnitude distinction is observed. The striking difference between values of $\varepsilon_{33}^{*\sigma}$ at $m > 0.2$ (see, e.g., curves 1, 3 and 5 in Fig. 2 (*f*)) is related to the difference between values of $\varepsilon_{33}^{*\xi}$ (Fig. 2 (*e*)) and the considerable piezoelectric effect as a result of the SC inclusions. On increasing the volume fraction of SC *m*, absolute values of the piezoelectric coefficients $|e_{3j}^{*}|$ and $|d_{3j}^{*}|$ increase monotonically (see, e.g., Fig. 2 (*a*) and (*b*)) and, therefore, the difference $\varepsilon_{33}^{*\sigma} - \varepsilon_{33}^{*\xi}$ in accordance with Eq. (9) increases. The difference between values of k_{33}^{*} (Fig. 2 (*g*)) is primarily due to the difference between $\varepsilon_{33}^{*\sigma}$ (Fig. 2 (*f*)) and d_{33}^{*} (Fig. 2 (*b*)). Of specific interest are curves of $g_{33}^{*}(m)$ shown in Fig. 2 (*c*). The volume-fraction dependence of the piezoelectric coefficient $g_{33}^{*}(m) = d_{33}^{*}(m) / \varepsilon_{33}^{*\sigma}(m)$ is non-monotonic and is due to the combination of the piezoelectric $d_{33}^{*}(m)$ and dielectric ($\varepsilon_{33}^{*\sigma}(m)$) properties (see Fig. 2 (*b*) and (*f*)). The location of $\max g_{33}^{*}(m)$ strongly depends on the aspect ratio ρ of the inclusions: at ρ = 0.1, when the highly prolate SC inclusions in the polymer matrix give rise to a slight depolarising effect, $\max g_{33}^{*}(m)$ is found in the range $0 < m < 0.05$, and on increasing ρ, when the depolarising effect becomes stronger and dielectric permittivity $\varepsilon_{33}^{*\sigma}(m)$ increases slower, $\max g_{33}^{*}(m)$ shifts towards the larger values of *m*. Considerable piezoelectric sensitivity of composite 1 (g_{33}^{*} > 200 mV·m / N, i.e., about 6 times more than $g_{33}^{(1)}$ of PMN–0.33PT SC [9]) is attained in the presence of inclusions with ρ = 0.1 at volume fractions $m \le 0.1$ (Fig. 2 (*c*)).

Results on the effective electromechanical properties of composites 2 and 3 (Figs. 3 and 4) suggest that the piezoelectric coefficients X_{33}^{*} and electromechanical coupling factor k_{33}^{*} show

small differences when comparing the data obtained using the EMM, FEM and EFM. For example, a difference between the aforementioned parameters calculated using different methods at $0 < m < 0.5$ and $0.1 \le \rho \le 0.5$ remains under 3 % for composite 2. In composite 3, a difference between the EFM and FEM data is less than 1 % in the same m and ρ ranges. This good agreement is attained when a moderate re-distribution of internal electric and mechanical fields in composites 2 and 3 takes place and electromechanical constants of their components are of similar order-of-magnitude. It is seen that the presence of a porous ceramic matrix with the anisotropy of the piezoelectric coefficients $e_{33}^{(2)} / |e_{31}^{(2)}| > 10$ does not lead to considerable differences between the values of X_{33}^{*} obtained using the EMM and FEM (Fig. 4).

Composites 1 – 3 studied in this work are also of interest due to the leading role of the longitudinal piezoelectric effect in forming the interconnections between the elastic, piezoelectric and dielectric properties. The presence of the highly piezo-active prolate SC inclusions, irrespective of the piezoelectric properties of the matrix surrounding them, enables one to simplify links between the piezoelectric coefficients from Eqs. (5)–(8) and interconnections between effective constants in Eqs. (9)–(12). To show the role of the longitudinal piezoelectric coefficients X_{33}^{*}, we introduce ratios $R_1 = d_{33}^{*} e_{33}^{*} / (\varepsilon_{33}^{*\sigma} - \varepsilon_{33}^{*\xi})$, $R_2 = e_{33}^{*} s_{33}^{*E} / d_{33}^{*}$, $R_3 = h_{33}^{*} s_{33}^{*D} / g_{33}^{*}$, and $R_4 = k_t^{*} / k_{33}^{*}$ and an anisotropy factor $\zeta_e = e_{33}^{*} / e_{31}^{*}$. Volume-fraction dependences of R_i and ζ_e are shown in Fig. 5.

We see, that due to $R_1 > 0.9$ in different cases (see curves 1, 2, 5, and 6 in Fig. 5 (*a*)), the piezoelectric contribution from the longitudinal piezoelectric effect (i.e., the term $d_{33}^{*} e_{33}^{*}$) into the difference between dielectric constants $\varepsilon_{33}^{*\sigma} - \varepsilon_{33}^{*\xi} = d_{33}^{*} e_{33}^{*} + 2 d_{31}^{*} e_{31}^{*}$ can exceed 90 %. For composite 1 at $\rho = 0.1$ and composite 3, the equality $R_1 = R_2$ holds with an accuracy to 1 % (cf. Figs. 5 (*a*) and 5 (*b*)). For composites 1 – 3, the inequality $R_3 > R_1$ is valid in a wide volume-fraction range (cf. Figs. 5 (*a*) and 5 (*c*)). As a result, the piezoelectric coefficient g_{33}^{*} that describes

longitudinal sensitivity of the composite has a negligible contribution from the transverse electromechanical interaction between the SC inclusion and its surrounding matrix. It should be noted that a similar tendency is observed in composites with different matrices – from piezo-passive polymer to highly piezo-active ceramic, and irrespective of piezoelectric sensitivity of the matrices.

To understand the volume-fraction behaviour of $R_4(m)$ (Fig. 5 (*d*)), we note that $(k_t^* / k_{33}^*)^2 = [(e_{33}^*)^2/ (c_{33}^{*D}\, \varepsilon_{33}^{*\xi})] / [(d_{33}^*)^2/ (s_{33}^{*E}\, \varepsilon_{33}^{*\sigma})]$, and this expression can be simplified due to equalities $c_{33}^{*D} = c_{33}^{*E} / [1 - (k_t^*)^2]$, $\varepsilon_{33}^{*\xi} = \varepsilon_{33}^{*\sigma} [1 - (k_t^*)^2]$ [10, 28] and $d_{33}^* \approx e_{33}^*\, s_{33}^{*E}$ (at $R_2 \approx 1$, see, for instance, Fig. 5 (*b*)). Thus, we state that $R_4 \approx (c_{33}^{*E}\, s_{33}^{*E})^{-1/2}$. The presence of the composite matrices with various elastic properties (see Table 1) has a significant influence on the balance of elastic moduli of the composite. As a consequence, R_4 varies in a wide range and can be non-monotonic (Fig. 5 (*d*)) in the case of a large difference between elastic moduli of components. It is seen that the largest values of $R_4 \approx 0.9$ and condition

$$k_t^* \approx k_{33}^* \tag{13}$$

are attained in composite 1 at $\rho = 0.1$. It should be noted for comparison that Eq. (13) holds in 1–3 ferroelectric ceramic / polymer composites [32]. As follows from Fig. 5 (*e*), the dependence of $|\zeta_e(m)|$, that describes the piezoelectric anisotropy, decreases monotonically for composites 1 – 3, and the monotonic decrease is also observed for the ratios $R_1(m)$ and $R_2(m)$ (see Fig. 5 (*a*) and (*b*)). The reason for this correlation is the transverse piezoelectric response of the composites studied: on increasing the volume fraction *m* the electromechanical interaction between the SC inclusions becomes less sensitive so that the role of the piezoelectric coefficient $e_{31}^*(m)$ increases.

The mutual arrangement of the curves for composites at $\rho = 0.1$ and $\rho = 0.3$ (Fig. 5) suggests that the ratios R_j and anisotropy factor ζ_e undergo considerable changes for composite 1 only. This

can be accounted for by the large difference between electromechanical constants of the highly piezo-active SC and piezo-passive polymer components of composite 1. However in composites 2 and 3 (ceramic matrix), the difference between electromechanical constants remains relatively small, so that small changes in curves of $R_j(m)$ and $\zeta_e(m)$ are observed (see curves 3 and 4 or 5 and 6 in each graph of Fig. 5) on changing the aspect ratio ρ of the prolate SC inclusion.

3.2. Squared Figures of Merit

It is worth noting that squared figures of merit concerned with the longitudinal ($(Q_{33}^*)^2$) and hydrostatic ($(Q_h^*)^2$) piezoelectric effects both exhibit similar volume-fraction behaviour. This can be observed from the mutual arrangement of curves 1, 3, 5 and 2, 4, 6, respectively, in Fig. 6. In composite 1 the larger values of $(Q_{33}^*)^2$ and $(Q_h^*)^2$ (see curves 1 and 2 in Fig. 6) are attained at relatively low volume fractions of SC (m < 0.3). This is related to the important role of the piezoelectric coefficients g_{3j}^* in forming both $(Q_{33}^*)^2$ and $(Q_h^*)^2$. In contrast to composite 1, the larger values of $(Q_{33}^*)^2$ and $(Q_h^*)^2$ in composite 3 (see curves 5 and 6 in Fig. 6) are attained at relatively high volume fractions of SC, when the piezoelectric coefficients d_{3j}^* become comparable to those of the SC. It should be added that the values of $(Q_{33}^*)^2$ and $(Q_h^*)^2$ shown for composites 1 and 3 (Fig. 6) are comparable to those evaluated [2, 33] for the 0–3 modified $PbTiO_3$ ceramic / elastomer composite. The values of $(Q_h^*)^2$ predicted for composites 1 and 3 are larger than those for a 0–3 $PbTiO_3$-based composite [1], and this new result can be of value for hydrophone applications of the novel PMN–0.33PT-based composites.

4. Conclusions

In the present paper modelling and property predictions have been carried out within the

framework of the model of the 0–3 piezo-active composite with spheroidal SC inclusions in a large matrix (Fig. 1). The model concepts and methods for averaging the electromechanical properties (EMM, EFM and FEM) have been applied to the 0–3 and 0–3–0 composites based on relaxor-ferroelectric PMN–0.33PT SC with high piezoelectric activity ($d_{3j}^{(1)} \sim 10^3$ pC / N). The following three combinations of components have been analysed: piezo-active SC / piezo-passive polymer, piezo-active SC / piezo-active monolithic ceramic and piezo-active SC / piezo-active porous ceramic. For composites based on PMN–0.33PT SC the longitudinal piezoelectric coefficients X_{33}^* (X = e, d, g, and h) and electromechanical coupling factor k_{33}^* have been calculated using the EMM, EFM and FEM.

Large values of the piezoelectric coefficients d_{33}^* and g_{33}^* and squared figures of merit $(Q_{33}^*)^2$ and $(Q_h^*)^2$ are attainable in the studied composites due to the presence of the aligned prolate SC inclusions with the piezoelectric coefficients $d_{3j}^{(1)} \sim 10^3$ pC / N. Comparison of the piezoelectric coefficients and other parameters calculated by the EMM, EFM and FEM has been carried out for the studied composites, and reasons for differences between the calculated constants have been discussed. The role of the piezoelectric anisotropy of the 0–3-type composite in forming its electromechanical properties and piezoelectric sensitivity has been analysed in terms of ratios R_i introduced in this paper.

Acknowledgments

The authors would like to thank Prof. Dr. R. Stevens (University of Bath, UK), Prof. Dr. A.E. Panich and Prof. Dr. I.A. Parinov (Southern Federal University, Russia) for their continued interest in the research problems. This work was partially supported by the administration of the Southern Federal University (Project No. 11.1.09f on basic research), and this support is gratefully acknowledged by one of the authors (V.Yu.T.).

References

[1] E.K. Akdogan, M. Allahverdi, and A. Safari, Piezoelectric composites for sensor and actuator applications. *IEEE Trans. Ultrason., Ferroelec., a. Freq. Contr.* **52**, 746–775 (2005).

[2] V.Yu. Topolov and C.R. Bowen, *Electromechanical Properties in Composites Based on Ferroelectrics*. London: Springer, 2009.

[3] T. Ritter, X. Geng, K.K. Shung, P.D. Lopath, S.-E. Park, and T.R. Shrout, Single crystal PZN/PT-polymer composites for ultrasound transducer applications. *IEEE Trans. Ultrason., Ferroelec., a. Freq. Contr.* **47**, 792–800 (2000).

[4] K.C. Cheng, H.L.W. Chan, C.L. Choy, Q. Yin, H. Luo, and Z. Yin, Single crystal PMN–0.33PT / epoxy 1–3 composites for ultrasonic transducer applications. *IEEE Trans. Ultrason., Ferroelec., a. Freq. Contr*. **50**, 1177–1183 (2003).

[5] K. Ren, Y. Liu, X. Geng, H.F. Hofmann, and Q.M. Zhang, Single crystal PMN–PT / epoxy 1–3 composite for energy-harvesting application. *IEEE Trans. Ultrason., Ferroelec., a. Freq. Contr.* **53**, 631–638 (2006).

[6] F. Wang, C. He, Y. Tang, X. Zhao, and H. Luo, Single crystal $0.7Pb(Mg_{1/3}Nb_{2/3})O_3 - 0.3PbTiO_3$ / epoxy 1–3 piezoelectric composites prepared by the lamination technique. *Mater. Chem. Phys*. **105**, 273–277 (2007).

[7] L.E. Cross, Relaxor Ferroelecrics, in *Piezoelectricity: Evolutions and Future of Technology*, Eds. W. Heywang, K. Lubitz, and W. Wersing. Berlin and Heidelberg: Springer, 2008, pp.131–155.

[8] B. Noheda, Structure and high-piezoelectricity in lead oxide solid solutions. *Curr. Opinion Solid St. Mater. Sci*. **6**, 27–34 (2002).

[9] R. Zhang, B. Jiang, and W. Cao, Elastic, piezoelectric, and dielectric properties of multidomain $0.67Pb(Mg_{1/3}Nb_{2/3})O_3 - 0.33PbTiO_3$ single crystals. *J. Appl. Phys*. **90**, 3471–

3475 (2001).

[10] Y. Xu, *Ferroelectric Materials and Their Applications*. Amsterdam, London, New York, and Toronto: North-Holland, 1991.

[11] A.V. Krivoruchko and V.Yu. Topolov, On the remarkable performance of novel 2–2-type composites based on [011] poled $0.93Pb(Zn_{1/3}Nb_{2/3})O_3 - 0.07PbTiO_3$ single crystals. *J. Phys. D.: Appl. Phys*. **40**, 7113–7120 (2007).

[12] V.Yu. Topolov and A.V. Krivoruchko, Orientation effects in 2–2 piezocomposites based on $(1 - x)Pb(A_{1/3}Nb_{2/3})O_3 - xPbTiO_3$ single crystals (A = Mg or Zn), *J. Appl. Phys*. **105**, 074105–7 p. (2009).

[13] V.Yu. Topolov and A.V. Krivoruchko, Polarization orientation effect and combination of electromechanical properties in advanced $0.67Pb(Mg_{1/3}Nb_{2/3})O_3–0.33PbTiO_3$ single crystal/polymer composites with 2–2 connectivity. *Smart Mater. Struct*. **18**, 065011–11 p. (2009).

[14] V.Yu. Topolov, C.R. Bowen, S.V. Glushanin, and A.E. Panich, Electromechanical coupling in the novel 2–2 parallel-connected PMN–0.33PT single-domain crystal / polymer composite. *Ferroelectrics* **393**, 27–37 (2009).

[15] S.V. Bezus, V.Yu. Topolov, and C.R. Bowen, High-performance 1–3-type composites based on $(1 - x)\ Pb(A_{1/3}Nb_{2/3})TiO_3 - x\ PbTiO_3$ single crystals (A = Mg, Nb). *J. Phys. D: Appl. Phys*. **39**, 1919–1925 (2006).

[16] V.Yu. Topolov, A.V. Krivoruchko, P. Bisegna, and C.R. Bowen, Orientation effects in 1–3 composites based on $0.93Pb(Zn_{1/3}Nb_{2/3})O_3 - 0.07PbTiO_3$ single crystals. *Ferroelectrics* **376**, 140–152 (2008).

[17] V.Yu. Topolov, A.V. Krivoruchko, and C.R. Bowen, Maxima of effective parameters of novel piezo-composites based on relaxor-ferroelectric single crystals. *Ferroelectrics* **351**, 145–152 (2007).

[18] R.E. Newnham, D.P. Skinner, and L.E. Cross, Connectivity and piezoelectric – pyroelectric composites. *Mater. Res. Bull*. **13**, 525–536 (1978).

[19] M.L. Dunn, Micromechanics of coupled electroelastic composites: Effective thermal expansion and pyroelectric coefficients. *J. Appl. Phys*. **73**, 5131–5140 (1993).

[20] V.M. Levin, M.I. Rakovskaja, and W.S. Kreher, The effective thermoelectroelastic properties of microinhomogeneous materials. *Internat. J. Solids a. Struct*. **36**, 2683–2705 (1999).

[21] N. Fakri, L. Azrar, and L. El Bakkali, Electroelastic behavior modeling of piezoelectric composite materials containing spatially oriented reinforcements. *Internat. J. Solids a. Struct*. **40**, 361–384 (2003).

[22] T. Mori and K. Tanaka, Average stress in matrix and average elastic energy of materials with misfitting inclusions. *Acta Metall*. **21**, 571–574 (1973).

[23] C. Poizat and M. Sester, Effective properties of composites with embedded piezoelectric fibres. *Comput. Mater. Sci*. **16**, 89–97 (1999).

[24] J.H. Huang and W.-S. Kuo, Micromechanics determination of the effective properties of piezoelectric composites containing spatially oriented short fibers. *Acta Mater*. **44**, 4889–4898 (1996).

[25] M.L. Dunn and M. Taya, Electromechanical properties of porous piezoelectric ceramics. *J. Am. Ceram. Soc*. **76**, 1697–1706 (1993).

[26] COMSOL, Inc. *COMSOL Multiphysics™ User's Guide* (version 3.5a, 2008), http://www.comsol.com

[27] W. Hackbusch, *Multi-grid Methods and Applications*. Berlin: Springer, 1985.

[28] T. Ikeda, *Fundamentals of Piezoelectricity*. Oxford, New York, and Toronto: Oxford University Press, 1990.

[29] F. Levassort, M.P. Thi, H. Hemery, P. Marechal, L.-P. Tran-Huu-Hue L, and

M. Lethiecq, Piezoelectric textured ceramics: Effective properties and application to ultrasonic transducers. *Ultrasonics* **44**, e621–e626 (2006).

[30] F. Levassort, M. Lethiecq, D. Certon, and F. Patat, A matrix method for modeling electroelastic moduli of 0–3 piezo-composites. *IEEE Trans. Ultrason., Ferroelec., a. Freq. Contr*. **44**, 445–452 (1997).

[31] V.Yu. Topolov, P. Bisegna, and A.V. Krivoruchko, Features of electromechanical properties of 1–3 composites based on $PbTiO_3$-type ceramics. *J. Phys. D: Appl. Phys.* **41**, 035406–8 p. (2008).

[32] H.L.W. Chan and J. Unsworth, Simple model for piezoelectric ceramic / polymer 1–3 composites used in ultrasonic transducer applications. *IEEE Trans. Ultrason., Ferroelec., a. Freq. Contr.* **36**, 434–441 (1989).

[33] C.R. Bowen and V.Yu. Topolov, Piezoelectric sensitivity of $PbTiO_3$-based ceramic / polymer composites with 0–3 and 3–3 connectivity. *Acta Mater*. **51**, 4965–4976 (2003).

To the paper "Analysis of the Piezoelectric Performance of Modern 0–3-Type Composites Based on Relaxor-Ferroelectric Single Crystals" by V. Yu. Topolov, P. Bisegna, and C. R. Bowen

Table 1. Room-temperature elastic moduli c_{ab}^{E} (in 10^{10} Pa), piezoelectric coefficients e_{ij} (in C / m^2) and relative dielectric permittivities ε_{pp}^{ξ} / ε_0 of components

Components	c_{11}^{E}	c_{12}^{E}	c_{13}^{E}	c_{33}^{E}	c_{44}^{E}	c_{66}^{E}	e_{31}	e_{33}	e_{15}	$\frac{\varepsilon_{11}^{\xi}}{\varepsilon_0}$	$\frac{\varepsilon_{33}^{\xi}}{\varepsilon_0}$
Polydomain PMN–0.33PT SC [9]	11.5	10.3	10.2	10.3	6.9	6.6	–3.9	20.3	10.1	1434	680
Poled PMN–0.35PT ceramic [29]	14.67	8.84	9.68	14.78	2.99	2.92	–5.0	28.0	14.3	1650	2650
Poled PMN–0.35PT porous ceramic at m_p= 0.3 (calc.)	8.43	5.22	5.17	7.78	1.96	1.61	–1.54	16.0	8.71	1050	1540
Araldite [30]	0.78	0.44	0.44	0.78	0.17	0.17	0	0	0	4.0	4.0

Figure 1. Schematic of the 0–3 composite. The spontaneous polarisation vector $P_s^{(1)}$ of the inclusion is denoted by an arrow. a_1 and a_3 are semiaxes of the spheroidal inclusion, m and $1 - m$ are volume fractions of components.

Figure 2. Effective parameters calculated for composite 1 by means of the EMM, FEM and EFM: piezoelectric coefficients e_{33}^* ((*a*) in C / m^2), d_{33}^* ((*b*) in pC / N), g_{33}^* ((*c*) in mV·m / N), and h_{33}^* ((*d*) in GV / m), relative dielectric permittivities $\varepsilon_{33}^{*\xi} / \varepsilon_0$ (*e*) and $\varepsilon_{33}^{*\sigma} / \varepsilon_0$ (*f*), and electromechanical coupling factor k_{33}^* (*g*).

Figure 3. Effective parameters calculated for composite 2 by means of the FEM at $\rho = 0.1$ (*a*) and $\rho = 0.3$ (*b*). Piezoelectric coefficients e_{33}^* in C/m^2, d_{33}^* in pC/N, g_{33}^* in mV·m/N, and h_{33}^* in GV/m.

Figure 4. Effective parameters calculated for composite 3 by means of the EMM and FEM: piezoelectric coefficients e_{33}^* ((*a*) in C / m^2), d_{33}^* ((*b*) in pC / N), g_{33}^* ((*c*) in mV·m / N), and h_{33}^* ((*d*) in GV / m) and electromechanical coupling factor k_{33}^* (*c*). In graph (*c*) the FEM data are shown only because of small differences (less than 1 %) between the effective parameters calculated by means of the EMM and FEM in the wide volume-fraction range.

Figure 5. Ratios R_i and anisotropy factor ζ_e which have been calculated for composites 1, 2, and 3 by means of the FEM.

Figure 6. Squared figures of merit $(Q_{33}^*)^2$ and $(Q_h^*)^2$ (in 10^{-15} Pa^{-1}) which have been calculated using the FEM data on piezoelectric coefficients d_{3j}^* and g_{3j}^* of composites 1, 2, and 3.

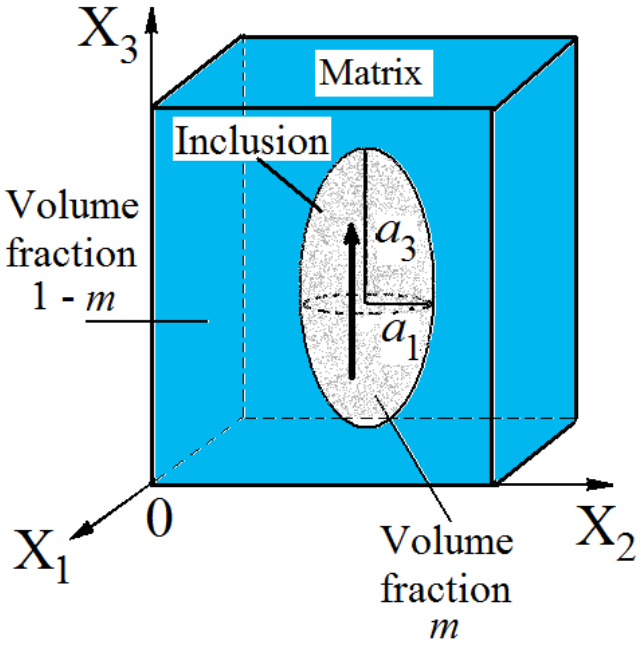
X3
Matrix
Inclusion
Volume
fraction
1 - m
a3
a1
0
X1
X2
Volume
fraction
m

Figure 1

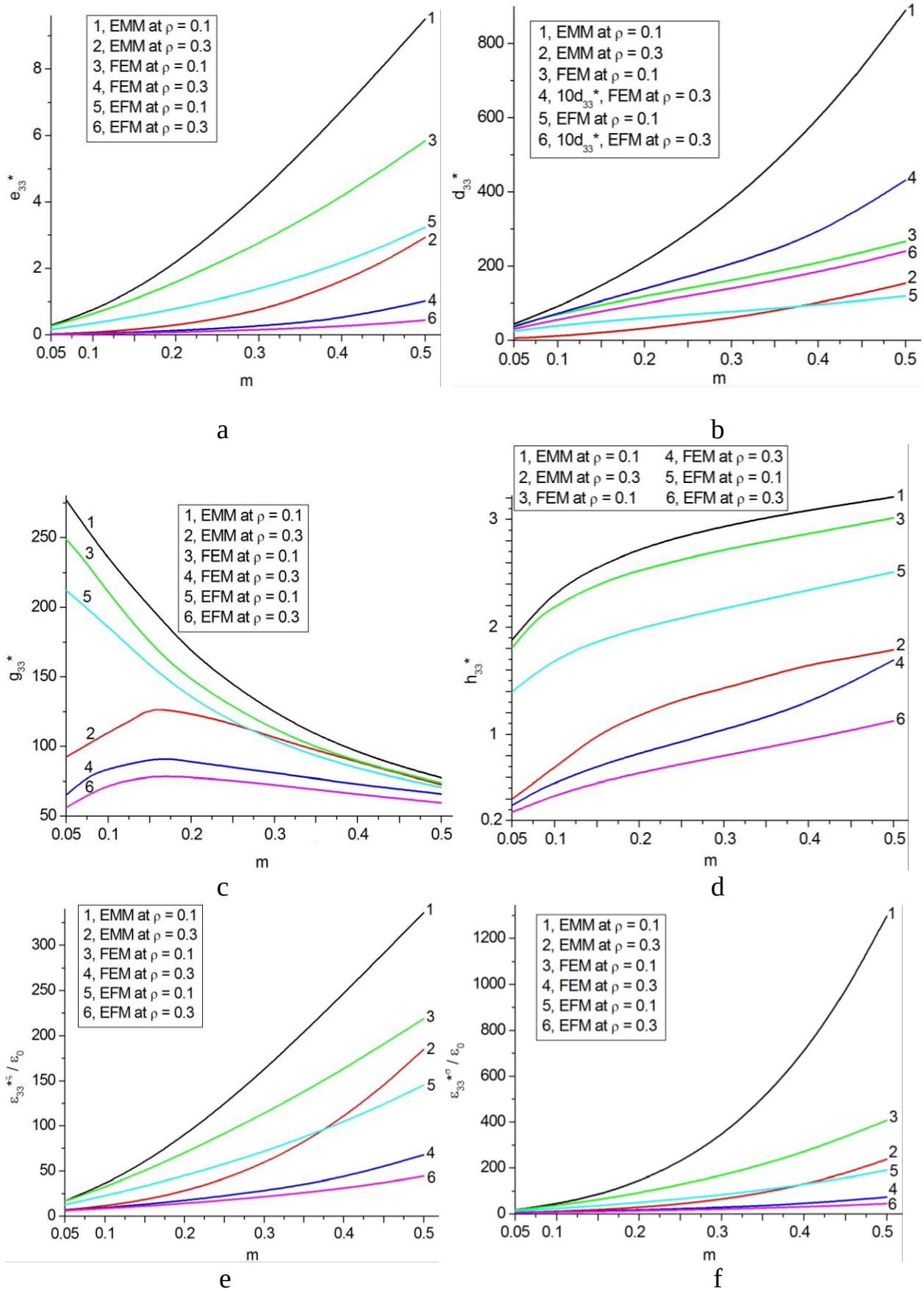

Figure 2 ***(continued)***

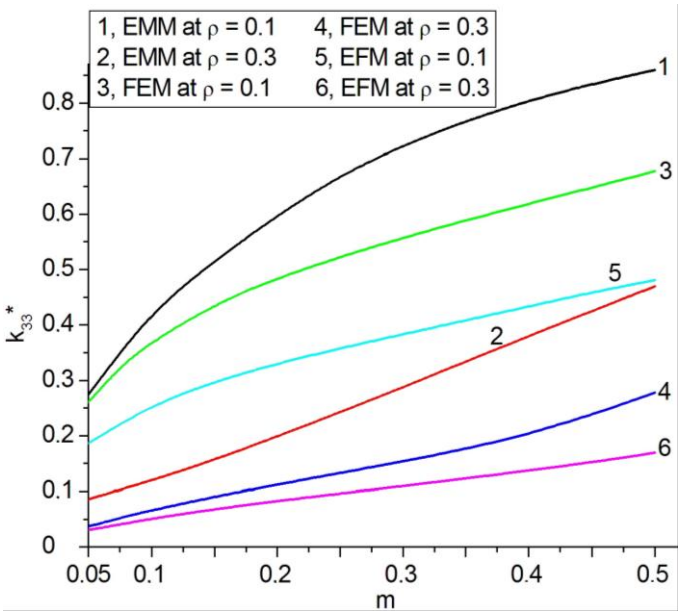
1, EMM at ρ = 0.1
2, EMM at ρ = 0.3
3, FEM at ρ = 0.1
4, FEM at ρ = 0.3
5, EFM at ρ = 0.1
6, EFM at ρ = 0.3
k33*
m
0
0.1
0.2
0.3
0.4
0.5
0.6
0.7
0.8
0.05
0.1
0.2
0.3
0.4
0.5
1
2
3
4
5
6

g

Figure 2

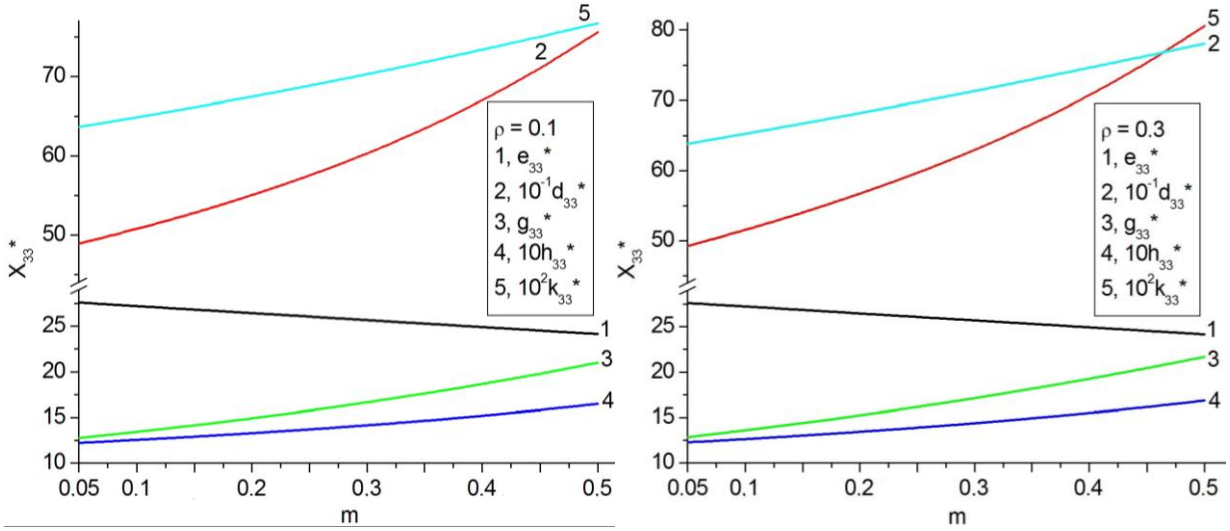
ρ = 0.1
1, e33*
2, 10-1d33*
3, g33*
4, 10h33*
5, 102k33*
X33*
m
ρ = 0.3
1, e33*
2, 10-1d33*
3, g33*
4, 10h33*
5, 102k33*
X33*
m

a b

Figure 3

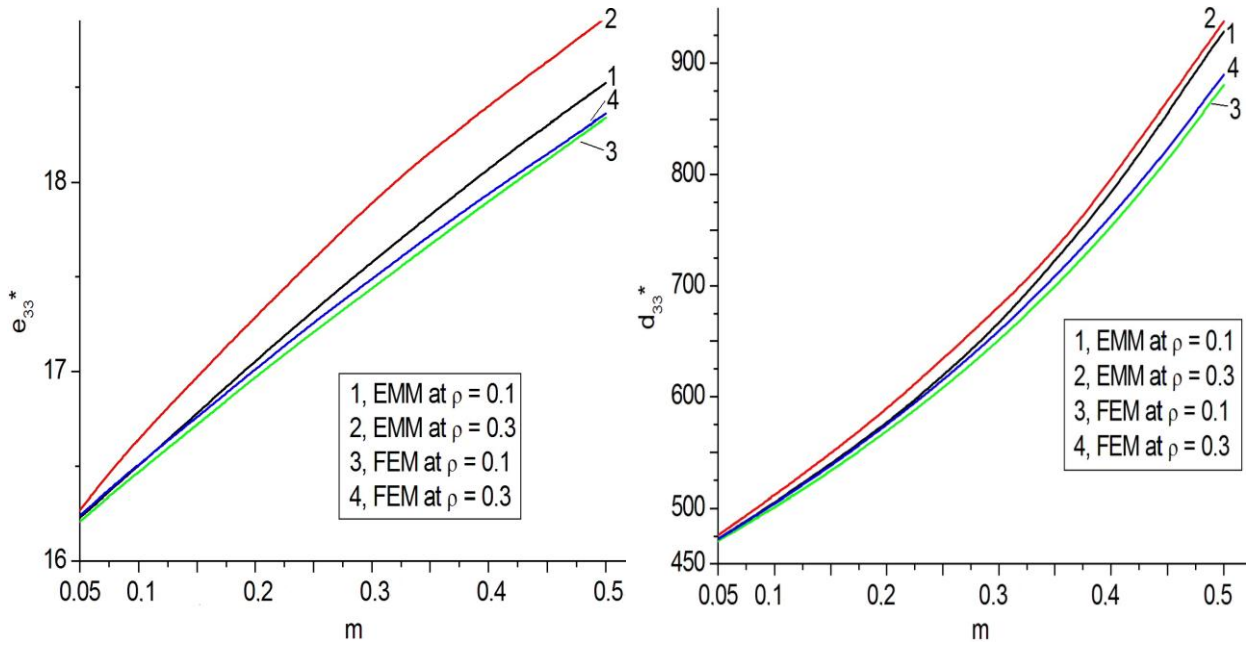

a

b

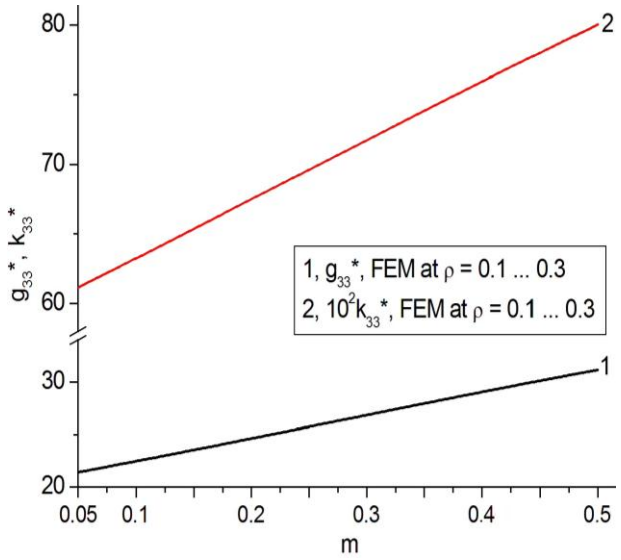

c

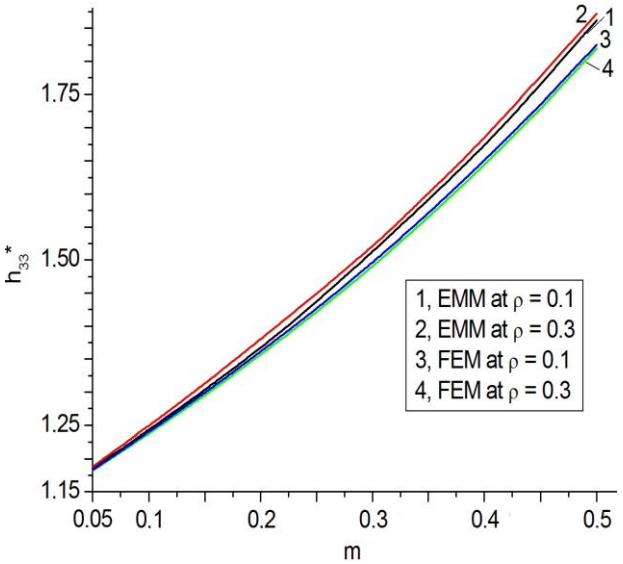

d

Figure 4

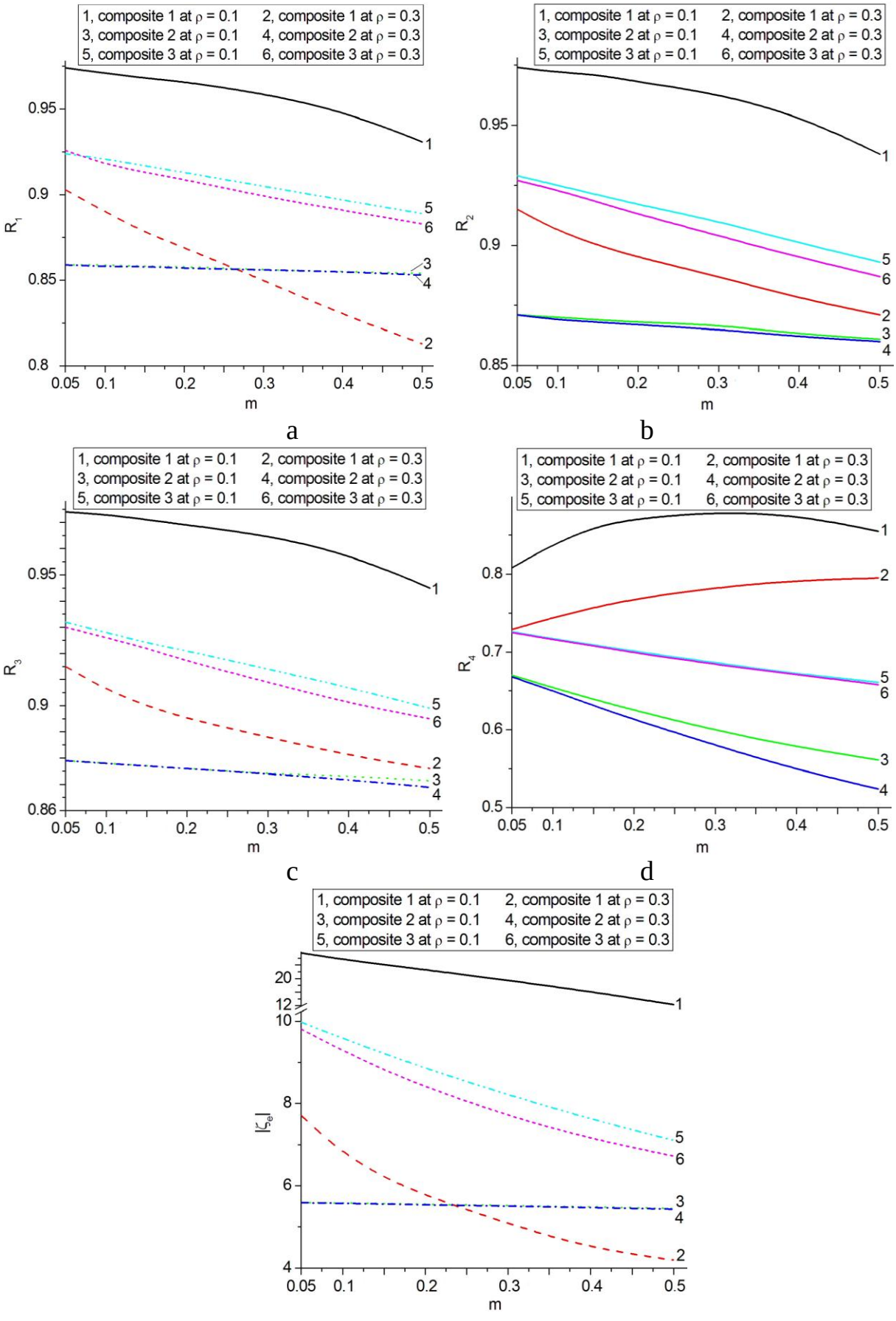
1, composite 1 at ρ = 0.1
2, composite 1 at ρ = 0.3
3, composite 2 at ρ = 0.1
4, composite 2 at ρ = 0.3
5, composite 3 at ρ = 0.1
6, composite 3 at ρ = 0.3
R1
R2
R3
R4
|ζe|
m
a
b
c
d
e

Figure 5

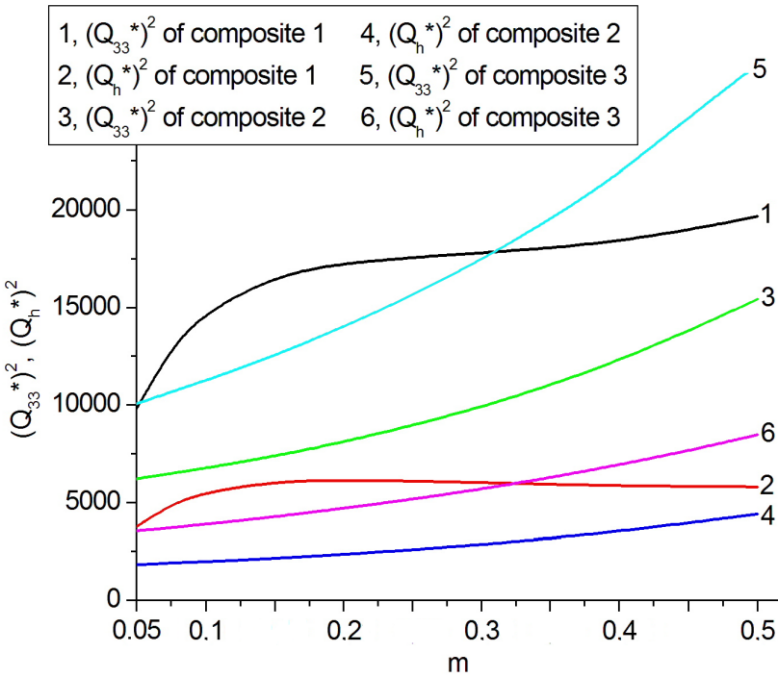
1, $(Q_{33}^*)^2$ of composite 1
2, $(Q_h^*)^2$ of composite 1
3, $(Q_{33}^*)^2$ of composite 2
4, $(Q_h^*)^2$ of composite 2
5, $(Q_{33}^*)^2$ of composite 3
6, $(Q_h^*)^2$ of composite 3
$(Q_{33}^*)^2$, $(Q_h^*)^2$
m
0
5000
10000
15000
20000
0.05
0.1
0.2
0.3
0.4
0.5
1
2
3
4
5
6

Figure 6